

Layout-Conditioned Autoregressive Text-to-Image Generation via Structured Masking

Zirui Zheng^{1,2}, Takashi Isobe^{1,†}, Tong Shen¹, Xu Jia^{2,†}, Jianbin Zhao², Xiaomin Li^{1,2}, Mengmeng Ge¹, Baolu Li², Qinghe Wang², Dong Li¹, Dong Zhou¹, Yunzhi Zhuge², Huchuan Lu², Emad Barsoum¹

¹Advanced Micro Devices Inc.

²Dalian University of Technology

{r1084, 1518272584, xml22, baoluli, qinghewang}@mail.dlut.edu.cn, {takashi.isobe, T.Shen, Mengmeng.Ge, d.li, Dong.Zhou, Emad.Barsoum}@amd.com, {xjia, zgyz, lhchuan}@dlut.edu.cn

Abstract

While autoregressive (AR) models have demonstrated remarkable success in image generation, extending them to layout-conditioned generation remains challenging due to the sparse nature of layout conditions and the risk of feature entanglement. We present Structured Masking for AR-based Layout-to-Image (SMARLI), a novel framework for layout-to-image generation that effectively integrates spatial layout constraints into AR-based image generation. To equip AR model with layout control, a specially designed structured masking strategy is applied to attention computation to govern the interaction among the global prompt, layout, and image tokens. This design prevents mis-association between different regions and their descriptions while enabling sufficient injection of layout constraints into the generation process. To further enhance generation quality and layout accuracy, we incorporate Group Relative Policy Optimization (GRPO) based post-training scheme with specially designed layout reward functions for next-set-based AR models. Experimental results demonstrate that SMARLI is able to seamlessly integrate layout tokens with text and image tokens without compromising generation quality. It achieves superior layout-aware control while maintaining the structural simplicity and generation efficiency of AR models.

Introduction

The success of AR modeling in Large Language Models (LLMs) (Touvron et al. 2023; Yang et al. 2025) has inspired many methods that extend AR principles to image generation tasks (Ramesh et al. 2021; Yu et al. 2021; Sun et al. 2024; Xie et al. 2024; Wang et al. 2024b; Tian et al. 2024), showcasing the effectiveness of AR-based generative frameworks in the vision domain. These approaches reformulate image generation as a next-token prediction, next-set prediction, or next-scale prediction task, demonstrating remarkable potential and emerging as strong competitors to diffusion models. In this work, we focus on exploring the potential of AR models in Layout-to-Image (L2I) generation.

The L2I generation conditions on the spatial locations and semantic descriptions of entities, and has been extensively explored in diffusion models based on different ar-

chitectures, including U-Net (Wang et al. 2022; Li et al. 2023; Zhou et al. 2024; Cheng et al. 2024; Wang et al. 2024a; Jia et al. 2024; Feng et al. 2024; Dahary et al. 2024; Yang et al. 2024) and Multimodal Diffusion Transformers (MMDiT_s) (Lee, Yoon, and Sung 2024; Zhang et al. 2024).

Most existing methods focus on integrating the layout modality with image and text modalities. They typically achieve this either by introducing additional blocks, or by directly manipulating attention maps and image latents in a training-free manner. However, extending such conditional controls to AR models is non-trivial due to two key challenges: (1) integrating precise layout conditions with text and image tokens while maintaining the simplicity of the AR architecture and avoiding the introduction of computationally expensive components; and (2) encoding bounding box descriptions and coordinates into layout tokens that remain compatible with AR models.

As for AR-based conditional image generation, there have been several works exploring along this direction (Li et al. 2024c,b; Yao et al. 2024; Chen et al. 2025b; Mu, Vasconcelos, and Wang 2025; Chung et al. 2025). However, most of these methods primarily rely on spatially aligned conditions, such as edge maps, depth maps, or semantic segmentation masks. These approaches can be broadly divided into two categories. The first category, inspired by Control-Net (Zhang, Rao, and Agrawala 2023), incorporates encoded visual conditions into the feature space alongside image tokens within AR models for later integration. However, layout conditions are inherently sparse, which can not provide many visual cues and priors like edges, depth maps, and semantic maps. In addition, each box corresponds to a description in the layout condition, which poses a challenge to such way of incorporating the boxes and descriptions simultaneously. The second category simply concatenates the conditional images with the text prompt and uses such tailored input to better accommodate AR models. However, most AR models are designed to process tokens of the same modality jointly, which leads to interference among regions or bounding boxes when applied to layout conditions that involve both bounding boxes and textual descriptions anchored to specific spatial locations. This interference hampers layout-aware control, particularly in complex scenes with numerous

Work done during an internship at AMD.

† Corresponding author. † Project lead.

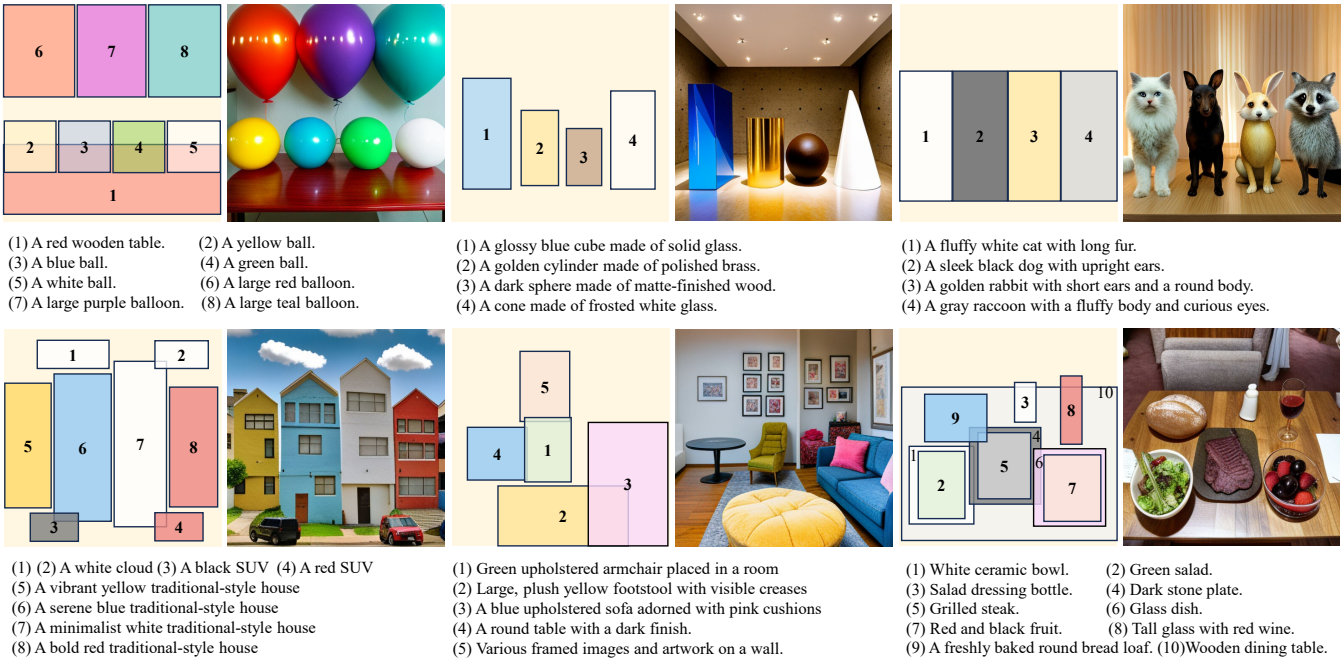


Figure 1: Example L2I generation results by SMARLI. We show that SMARLI could achieve fine-grained controllable generation with accurate spatial location control and precise rendering of complex attributes, including color, shape, and texture. The global text prompt is omitted for brevity.

objects and diverse attributes, as shown in Fig. 1.

In this work, we propose SMARLI, a layout-conditioned AR image generation framework that incorporates a structured masking strategy and a layout-conditioned GRPO-based post-training scheme tailored for next-set-based AR models.

Specifically, we first encode the global text prompt, layout condition, and image using respective tokenizers and concatenate the resulting tokens into a unified input token sequence. This input sequence is then fed into the AR transformer, where a structured masking strategy is designed to control attention computation across different token types in the transformer architecture. Layout tokens are designed to attend to both global text prompts for incorporating broader context and local layout context within the same region, while being masked from other regions to prevent information interference. Image tokens receive guidance from both global semantic prompts and region-specific layout tokens, ensuring the generation process being controlled by appropriate contexts while avoiding attribute confusion. This introduces inductive priors that align with the sequential organization of prompt, layout, and image tokens, facilitating efficient training without requiring considerable architectural modifications to the base AR models. To further improve generation quality and layout accuracy, we propose a GRPO-based post-training (Shao et al. 2024) scheme tailored for next-set AR models. The human preference score is introduced as a reward to improve image quality, and a layout reward is designed to enhance layout control. Extensive experiments demonstrate the effectiveness of the pro-

posed framework in AR-based layout-to-image generation. It performs favorably against state-of-the-art diffusion-based counterparts, showing further potential of AR models.

The main contribution of this paper can be summarized as follows: (1) to the best of our knowledge, we are the first to explore a layout conditioned AR framework for text-to-image (T2I) generation, which performs favorably against diffusion-based counterparts; (2) we propose SMARLI, a novel layout-conditioned AR image generation framework that incorporates a structured mask strategy to effectively inject layout signals into the generation process, mitigating region-description misalignment; (3) a GRPO-based post-training scheme is introduced for next-set-based AR models and we propose a novel layout reward and integrate it with an existing image quality reward to jointly improve image quality and layout controllability.

Related work

Autoregressive Image Generation

AR models have recently achieved image generation performance comparable to diffusion models. Typically, they employ a discrete VQ-VAE tokenizer (Esser, Rombach, and Ommer 2021) to convert images into sequences of tokens, which are then modeled using next-token prediction in raster-scan order (Sun et al. 2024; Wang et al. 2024b; Chen et al. 2025a). To enhance both efficiency and output quality, recent approaches have reformulated the generation process. Masked generative models (Chang et al. 2022, 2023; Xie et al. 2024; Li et al. 2024a; Deng et al. 2024) leverage bidirectional context to predict sets of masked tokens in parallel,

while still maintaining AR training. VAR (Tian et al. 2024) introduces residual vector quantization to enable next-scale prediction, further improving image quality.

Meanwhile, conditional image generation in AR models is still in its early stages. ControlAR (Li et al. 2024c) and CAR (Yao et al. 2024) extract and fuse condition image features with image tokens. ControlVAR (Li et al. 2024b) jointly decodes the image and the condition to establish a connection. EditAR (Mu, Vasconcelos, and Wang 2025) simply appends the condition image with a different position embedding to the input sequence. ContextAR (Chen et al. 2025b) further introduces a cross-condition mask and learnable position embeddings to unify multiple condition images in the input sequence. TwFA (Yang et al. 2022) and LayoutEnc (Cui et al. 2025) have explored category-based layout control. In this paper, we propose SMARLI, the first AR T2I framework that seamlessly incorporates the global text prompt and layout conditions.

Layout-conditioned T2I Generation

For layout control, existing diffusion-based T2I models often achieve effective layout control (Li et al. 2023; Wang et al. 2024a; Cheng et al. 2024; Chen, Laina, and Vedaldi 2024; Yang et al. 2024; Ge et al. 2024; Dahary et al. 2024) by introducing additional attention between the layout and image or directly manipulating the attention map and image latent. For instance, GLIGEN incorporates layout conditions into newly introduced trainable layers through a gated mechanism. InstanceDiffusion extends this paradigm to instance-level control, supporting flexible layout specifications. HiCo employs a multi-branch structure to achieve precise layout control through hierarchical layout modeling. SiamLayout employs a separate branch of the network to process the layout in MMDiT. RPG independently generates each region and composes them in the image latent space based on a pre-defined coarse layout. However, no existing AR-based T2I model has effectively achieved precise layout control when both the prompt and layout are used as conditions.

In this paper, we propose a structured masking strategy to realize effective layout control under the unified input sequence paradigm without introducing computationally expensive components, filling the gaps in previous research.

Post-training in Visual Content Generation

The success of reward-based optimization in text-to-image (T2I) generations (Clark et al. 2023; Xu et al. 2023) has motivated extensive research into enhancing model performance through feedback mechanisms. Early pioneering works established the foundation by applying reinforcement learning techniques to diffusion models, with DDPO (Black et al. 2023) employing RL for finetuning and Diffusion-DPO (Wallace et al. 2024) adopting Direct Preference Optimization (DPO) (Rafailov et al. 2023) to align models with human preferences. Building on these advances, recent methods have expanded reward-based optimization across different architectures and objectives. For diffusion models, FlowGRPO (Liu et al. 2025) and DanceGRPO (Xue et al. 2025) have extended GRPO to boost visual content

generation, while ReNeg (Li et al. 2025) focuses on optimizing negative prompt embeddings through reward feedback tuning. In the next-token-based AR T2I domain, SimpleAR (Wang et al. 2025) and T2I-R1 (Jiang et al. 2025) have demonstrated notable progress in text-image alignment by employing GRPO for post-training. However, GRPO has not yet been explored in next-set-based AR T2I models, and its application to L2I generation remains an open question. To address this gap, a GRPO-based post-training scheme is introduced for next-set-based AR models, and a specialized layout reward is proposed to effectively integrate GRPO-based post-training strategies into layout-conditioned generation. Complemented by an existing image quality reward, this post-training scheme enables more effective layout control while improving generation quality.

Preliminary

Next-set AR

Traditional AR models generate images token-by-token in raster order, leading to inefficiency for high-resolution images due to long sequences. Next-set AR models address this by predicting a set of image tokens at each timestep, reformulating image generation as masked token prediction. Specifically, during inference, all image tokens are initially masked, and at each time step, the model predicts a subset of tokens in parallel. Masked tokens are progressively revealed following a scheduling strategy that reduces the masking ratio from 1.0 to 0.

GRPO

GRPO-based post-training requires a trainable policy model π_θ , a behavior policy model $\pi_{\theta_{old}}$, and a frozen reference model π_{ref} that are all initialized using the checkpoint obtained from prior supervised fine-tuning (SFT). Given condition c , the behavior policy model $\pi_{\theta_{old}}$ samples a group of outputs o_1, o_2, \dots, o_G , and then optimizes the following objective to update π_θ .

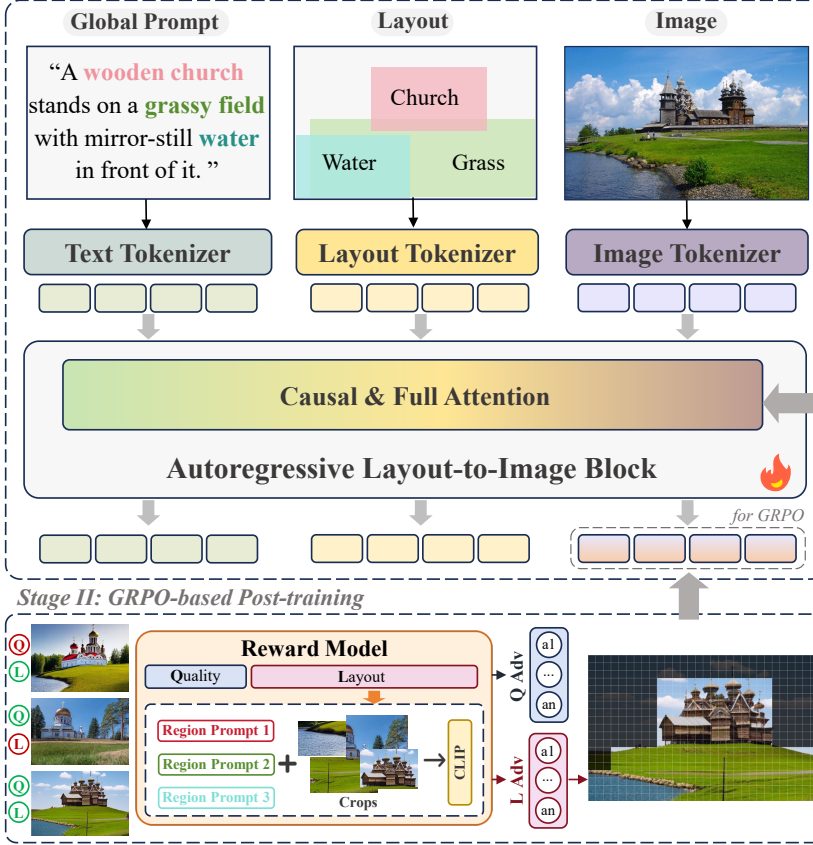
$$\mathbb{E} \left[\frac{1}{G} \sum_{i=1}^G \frac{1}{|o_i|} \sum_{t=1}^{|o_i|} \{ \min(r_{i,t} A_{i,t}, \hat{r}_{i,t} A_{i,t}) - \beta D_{KL} \} \right], \quad (1)$$

where $r_{i,t} = \frac{\pi_\theta(o_{i,t}|c, o_{i,<t})}{\pi_{\theta_{old}}(o_{i,t}|c, o_{i,<t})}$ denotes the importance sampling ratio between the current policy π_θ and the behavior policy $\pi_{\theta_{old}}$, while $\hat{r}_{i,t} = \text{clip}(r_{i,t}, 1 - \epsilon, 1 + \epsilon)$ applies a clipping threshold ϵ to stabilize training. $A_{i,t}$ represents the advantage of t -th token of o_i computed within group, and the KL divergence $D_{KL} = D_{KL}(\pi_\theta \parallel \pi_{ref})$, weighted by coefficient β , regularizes the updated policy towards a fixed reference policy π_{ref} to reduce overfitting.

Method

We build our framework upon Show-o (Xie et al. 2024), which follows the next-set prediction paradigm and serves as a foundational approach in AR image generation. As shown in Fig. 2, our framework consists of three main components:

Stage I: Supervised Fine-tuning



Layout Tokenization

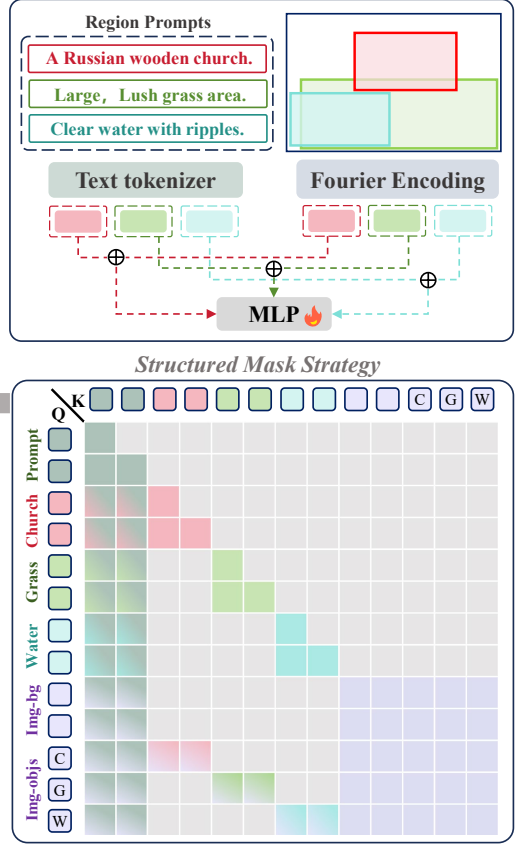


Figure 2: An overview of the proposed framework. In stage 1, the global prompt and image are tokenized using Show-o’s original setup. Layout tokens are derived from the layout tokenizer based on the bounding boxes and region prompts. A unified input sequence, formed by the three types of tokens, is fed into the transformer equipped with a dedicated structured masking strategy to enable more effective layout control. After SFT, we further introduce a GRPO-based post-training stage to improve the layout controllability and image quality simultaneously with a dedicated layout reward and image quality reward.

(1) **Tokenization**: The global text prompt, layout, and image are tokenized separately, concatenated into a single sequence, and fed into the AR transformer. (2) **Layout control with structured masking strategy**: To equip the AR model with more effective layout control, a specially designed structured masking strategy is applied to attention computation. (3) **Layout GRPO**: To further improve the generation quality and layout accuracy, a GRPO-based post-training stage is adapted to the next-set AR model with an additional layout reward.

Tokenization

For the prompt and image, we adopt Show-o’s setup: the prompt is tokenized by Show-o’s text tokenizer, and the image is tokenized into discrete tokens in the same way as MAGVITv2 (Yu et al. 2023).

Layout condition consists of multiple objects, where each object is defined by a bounding box $obj_i^{box} = [x_0, y_0, x_1, y_1]$ and a textual description obj_i^{text} . The box specifies the normalized top-left and bottom-right coordinates, while the text

provides the semantic description of the object.

Inspired by TwFA (Yang et al. 2022), we directly use Show-o’s text tokenizer E and codebook C to encode the region description of the layout. Then, each bounding box is represented as a set of Fourier embeddings. The text tokens and box tokens are concatenated into a longer sequence and passed through a zero-initialized MLP with a residual connection, as shown in the Layout Tokenizer in Fig. 2.

$$x_i = \text{Concat}(C(E(obj_i^{text})), \text{Fourier}(obj_i^{box})) \quad (2)$$

$$obj_i^{\text{layout}} = x_i + \text{MLP}(x_i) \quad (3)$$

The layout tokens of object i can be expressed as the above equations, where Concat denotes concatenation in the sequence dimension. Finally, the input to the AR transformer is a sequence composed of prompt, layout, and image tokens, where the image tokens are partially replaced by [MASK] tokens for SFT training.

Layout Control with Structured Masking Strategy
As shown in Fig. 2, given a sequence of tokens for the prompt, layout, and image tokens in order, a specially de-

signed structured masking strategy is applied to attention computation in transformer blocks as follows.

As for the global text prompt tokens, we adopt the standard causal masking strategy used in Show-o. For the layout tokens, they are encouraged to attend to both the global text prompt tokens and the layout tokens belonging to the same object. On one hand, allowing layout tokens to attend to the global prompt helps incorporate contextual information in the layout token representation in the stacked transformer blocks. This could avoid the model focusing on local details while missing the big picture when accumulating information in layout tokens. The global prompt could provide much information about the relationship between a certain region and the whole image. On the other hand, as for the subset of layout tokens of the same object, a standard causal mask is applied to them. In this way, these layout tokens could accumulate fine-grained spatial and attribute information within a certain region. For layout tokens belonging to other regions, the masks are designed to isolate them from each other to avoid information interference.

For image tokens, they attend to two subsets of preceding tokens: the global prompt tokens, which provide semantic guidance, and the layout tokens corresponding to the region they fall into. If an image token lies within multiple overlapping object boxes, it attends to all associated layout tokens to capture composite layout semantics. In this way, the generation process of image tokens is steered by global semantic guidance and associated layout conditions, ensuring precise alignment while reducing confusion from irrelevant content.

Together, these strategies introduce a structured inductive prior that aligns with the sequential organization of prompt, layout, and image tokens, facilitating efficient training without introducing notable architectural modifications or significant parameter overhead.

Layout-GRPO

As mentioned in the *Preliminary* section, Show-o adopts a *next-set prediction* fashion, at each time step it computes attention over the whole image token sequence but only retains a subset of tokens with high confidence as prediction. The prediction at each step is considered an action in RL.

GRPO-based post-training relies on estimating and optimizing policy distributions through computing log-probabilities of generated sequences including $\pi_\theta(o_{i,t}|c, o_{i,<t})$, $\pi_{\theta_{old}}(o_{i,t}|c, o_{i,<t})$, and $\pi_{\theta_{ref}}(o_{i,t}|c, o_{i,<t})$. Adapting GRPO to next-set-based AR models for image generation poses unique challenges. While this computation is straightforward in standard AR models through sequential factorization, next-set-based AR models lack this natural decomposition due to their iterative, non-sequential generation process, where multiple tokens are predicted simultaneously at each step. To address this challenge and optimize the policy model, we begin by using $\pi_{\theta_{old}}$ to perform the rollout stage, during which we record the predicted logits along with their corresponding spatial locations, as well as the input tokens at each time step. Subsequently, the π_θ and $\pi_{\theta_{ref}}$ could traverse the same rollout trajectory through step-wise forward passes to compute the corresponding policy distributions.

During the post-training stage with GRPO, we use HPSv2.1 (Wu et al. 2023) as a reward to improve image quality. However, we observe that using only the image quality reward causes the GRPO-based post-training to degrade the layout control capability acquired during the SFT stage. To address this, we propose a dedicated **layout reward**.

Specifically, we introduce a simple yet effective reward design. For each bounding box in the layout conditions, the corresponding region is cropped out and CLIP similarity between the cropped patch and the corresponding description is computed. The layout reward is then computed as the average of CLIP similarity scores over all conditioned regions. On one hand, it would examine the existence of semantic categories in the region and encourage the model to actually generate the correct things and stuff; on the other hand, it would examine whether the region has the color, texture, and shape in the descriptions and encourage the correct alignment between attribute description and generation.

$$A_{i,t} = \omega^{\text{hps}} \cdot A_i^{\text{hps}} + \omega^{\text{layout}} \cdot A_i^{\text{layout}} \quad (4)$$

The overall advantage is defined in Eq. 4 as a weighted combination of the HPS advantage A_i^{hps} , which reflects image quality, and the layout advantage A_i^{layout} , which reflects layout control capability. Additionally, we apply a larger ω^{layout} to the layout advantage of image tokens that lie within the bounding boxes specified by the layout condition. This targeted enhancement encourages the model to focus more on layout-aligned regions during policy optimization.

Experiments

Datasets and Evaluation Metrics

LayoutSAM (Zhang et al. 2024) is a large-scale layout dataset containing 2.7 million image-text pairs and 10.7 million entities. Each entity is annotated with a bounding box and a detailed textual description, generated through automated annotation methods to obtain detailed descriptions.. The companion set, LayoutSAM-Eval, is designed to evaluate layout-to-image generation quality.

For **SFT training**, we randomly sample approximately 1M instances from the training split of LayoutSAM, constrained by limited computational resources. For **GRPO-based post-training**, we further filter the SFT data by removing samples containing semantically redundant instances. Specifically, we leverage Qwen3-14B (Yang et al. 2025) to analyze overlapping bounding boxes and exclude those with redundant object annotations, thereby enhancing the fidelity and reliability of the layout reward signals.

Evaluation is conducted on the LayoutSAM-Eval benchmark proposed in CreatiLayout (Zhang et al. 2024), following the same evaluation protocol. Layout control is assessed from two key perspectives: spatial positioning and attribute alignment. Spatial positioning measures how accurately objects are placed according to the given layout, while attribute alignment evaluates whether the color, texture, and shape of the generated image’s layout-controlled regions align with the corresponding layout conditions. The image quality is evaluated in terms of human preference

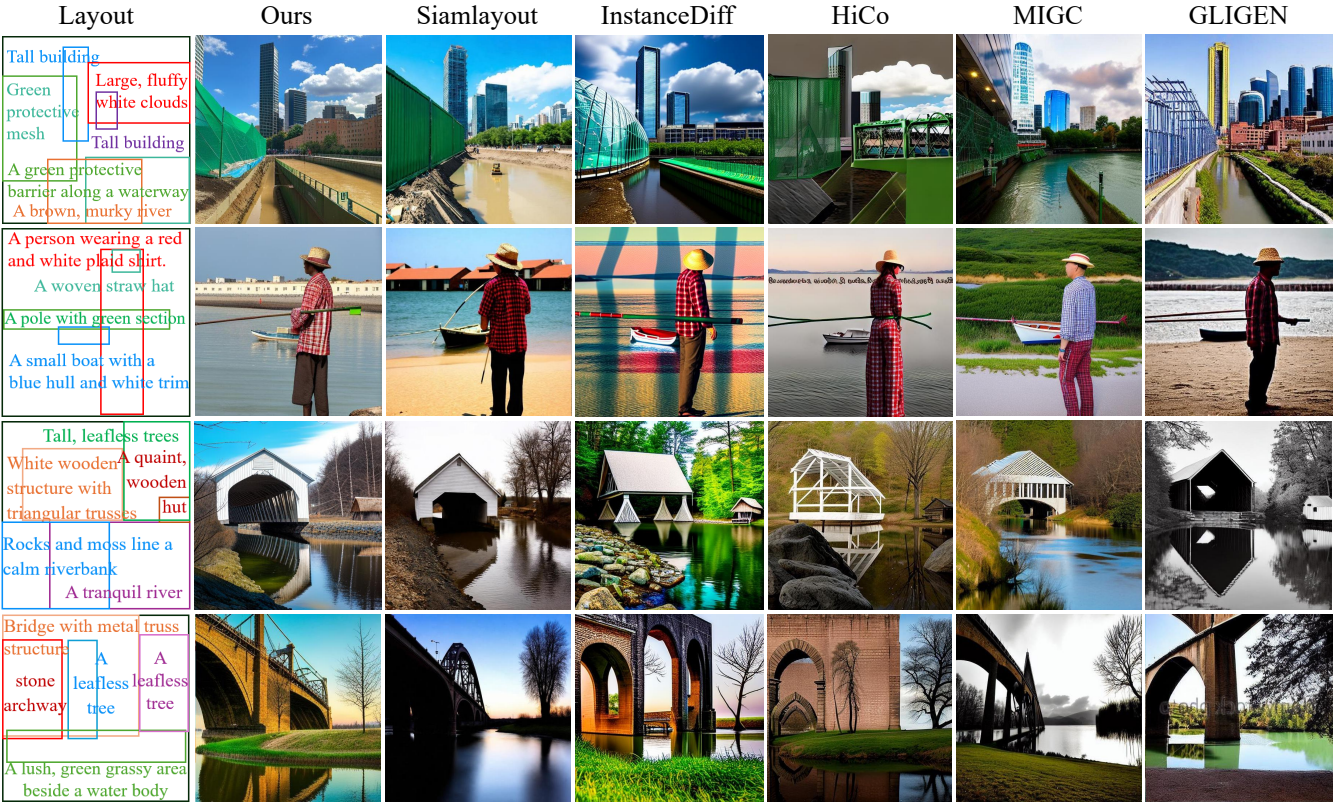


Figure 3: Qualitative results on the LayoutSAM-Eval. Conditioned on a complicated layout, prior works fail to faithfully generate all objects mentioned in the layout or accurately reflect specific attributes, such as the green protective barrier and the small boat with a blue hull and white trim.

(IR (Xu et al. 2023), Pick (Kirstain et al. 2023)), text-image alignment (CLIP (Radford et al. 2021)), and perceptual quality (FID (Heusel et al. 2017), IS (Salimans et al. 2016)).

Training Details

We adopt Show-o as the foundation model, with a training resolution of 512×512 . For the SFT stage, we use the AdamW (Loshchilov and Hutter 2017) optimizer with a fixed learning rate of 2×10^{-5} , training for 30,000 iterations with a batch size of 128. Trainable components include the entire AR transformer and the MLP in the layout tokenizer.

In GRPO-based post-training, we set the number of groups to 4, the generation time step to 10, the batch size to 28, and the learning rate to 1×10^{-4} , training for 100 iterations. We adopt LoRA (Hu et al. 2022) fine-tuning with rank 256 for the attention modules. For rollouts, we set the temperature to 1 and the classifier-free guidance (CFG) scale to 5, consistent with the T2I sampling settings in Show-o. Following the discussion in DanceGRPO (Xue et al. 2025) regarding the optimization bias introduced by CFG sampling, we adopt a fully on-policy training strategy. Specifically, in line with DanceGRPO, each policy update is based solely on fresh rollouts, and trajectories from previous rollouts are not reused. The β in Eq.1 is set to 0. The ω^{hps} and ω^{layout} are set to 1. When the image token lies within the bounding boxes

specified by the layout condition, ω^{layout} is set to 1.1.

Comparison with State-of-the-Arts

We compare SMARLI with state-of-the-art diffusion-based layout-to-image models, including GLIGEN (Li et al. 2023), Ranni (Feng et al. 2024), MIGC (Zhou et al. 2024), InstanceDiff (Wang et al. 2024a), Be Yourself (Dahary et al. 2024), HiCo (Cheng et al. 2024), and SiamLayout (Zhang et al. 2024). As SiamLayout-FLUX uses a much larger backbone with significantly more parameters, we report results for SiamLayout-SD3 only.

The quantitative results are presented in Tab. 1. The proposed SMARLI demonstrates strong layout control performance, excelling in spatial, color, texture, and shape control. It also achieves promising quality performance, with better FID and competitive results in IR, CLIP, and Pick. We believe this small quality gap could be further reduced by using a more advanced AR-based T2I foundation model.

The qualitative results are shown in Fig. 3. Images generated by our method demonstrate superior layout control, exhibiting more accurate spatial positioning and faithful attribute rendering than existing approaches. These results highlight the effectiveness of the proposed masking strategy, which enhances the semantic representation of layout tokens and mitigates interference between tokens from dif-

LayoutSAM-Eval	Layout Control				Image Quality				
	Spatial \uparrow	Color \uparrow	Texture \uparrow	Shape \uparrow	IR \uparrow	Pick \uparrow	CLIP \uparrow	FID \downarrow	IS \uparrow
Real Images	98.95	98.45	98.90	98.80	-	-	-	-	-
GLIGEN	77.53	49.41	55.29	52.72	-10.31	20.78	32.42	21.92	20.57
Ranni	41.38	24.10	25.57	23.35	-28.46	20.49	31.40	27.24	19.81
MIGC	85.66	66.97	71.24	69.06	-13.72	20.71	31.36	21.19	19.65
InstanceDiff	87.99	69.16	72.78	71.08	9.14	21.01	31.40	19.67	20.02
Be Yourself	53.99	31.73	35.26	32.75	-12.31	20.20	31.02	28.10	17.98
HiCo	87.04	69.19	72.36	71.10	12.36	21.70	32.18	22.61	20.15
SiamLayout	92.67	<u>74.45</u>	<u>77.21</u>	<u>75.93</u>	69.47	22.02	34.01	<u>19.10</u>	22.04
SMARLI	95.33	86.84	90.44	89.45	<u>69.08</u>	21.53	<u>33.12</u>	18.16	18.86

Table 1: Quantitative results on the LayoutSAM-Eval (Zhang et al. 2024). Bold, underline, and italic represent the best, second, and third best methods, respectively.

ferent objects, together with the benefits introduced by the well-designed layout reward in GRPO-based post-training. The compelling quantitative and qualitative results demonstrate the potential of AR models as strong competitors to diffusion models.

Ablation Study

Masking Strategy. We first conduct an ablation study on the effectiveness of the proposed masking strategy. The model without GRPO-based post-training (SMARLI-SFT) is used as the baseline, and the results are reported in Tab. 2. We examine two variant masking strategies: (1) layout tokens are isolated from global prompt tokens (w/o LP), causing them to lose access to the semantic context provided by the global prompt; (2) layout tokens are no longer treated as independent units per object but are instead processed as a whole (w/o Local Causal). We observe a significant performance degradation on both variants, as shown in Tab. 2.

For the first variant, prohibiting layout tokens from attending to global prompt tokens in the attention significantly undermines the model’s ability to control object attributes during layout-aware generation, highlighting the critical role of global prompt tokens in enriching layout token semantic representations. For the second variant, each layout token attends not only to the global prompt tokens but also to the preceding layout tokens. Moreover, image tokens are not strictly constrained to attend only to layout tokens whose designated spatial regions encompass them. This indiscriminate integration of attribute and spatial information from different objects leads to performance degradation, particularly in spatial positioning metrics, while the effect on attribute alignment is relatively minor. We attribute this to the fact that layout tokens still attend to the global prompt, preserving access to rich semantic information.

GRPO-based Post-training. We conduct a series of ablation studies starting from a supervised fine-tuning (SFT) baseline to evaluate the impact of the GRPO-based post-training stage. As shown in Tab. 3, applying HPS as the only reward enhances image quality but compromises layout consistency. The degradation is particularly evident in color

	Spatial \uparrow	Color \uparrow	Texture \uparrow	Shape \uparrow
SMARLI-SFT	95.26	86.17	89.79	88.56
w/o LP	<u>95.17</u>	79.83	84.35	82.74
w/o Local Causal	93.93	<u>83.22</u>	87.12	<u>85.68</u>

Table 2: Ablation study on different masking strategies.

HPS	Layout	Layout Control				Image Quality	
		Spatial	Color	Texture	Shape	IR	Pick
\times	\times	95.26	86.17	89.79	88.56	60.88	21.45
\checkmark	\times	94.47	85.10	89.27	88.09	72.16	21.74
\times	\checkmark	<u>95.29</u>	<u>86.75</u>	90.31	89.33	59.17	21.37
\checkmark	\checkmark	95.33	86.84	90.44	89.45	<u>69.08</u>	<u>21.53</u>

Table 3: Ablation study on GRPO-based post-training.

accuracy, likely due to HPS’s preference for specific color styles. To mitigate this issue, we introduce the layout reward that promotes alignment between the generated image and the input layout. While it improves layout controllability, it comes at the cost of reduced image quality. Finally, the combination of HPS and our layout reward enables the model to generate images with improved visual quality while achieving better layout alignment. Interestingly, incorporating the HPS reward on top of the layout reward further enhances layout controllability. This improvement can be attributed to the HPS reward complementing prompt-level consistency, thereby reinforcing overall layout adherence under the constraints imposed by the layout reward.

Conclusion

In this paper, we have presented SMARLI, a novel framework that effectively integrates layout constraints into autoregressive text-to-image generation. Our structured masking strategy addresses the challenges of sparse layout con-

ditioning and feature entanglement, enabling precise spatial control while preserving attribute coherence. Additionally, the GRPO-based post-training with image quality reward and the specialized layout reward enhances generation quality and layout fidelity. Experimental results demonstrate that SMARLI achieves superior layout control while maintaining the simplicity and efficiency of autoregressive models. This work provides valuable insights for incorporating layout conditions into autoregressive models, advancing the field of autoregressive-based controllable image generation.

References

Black, K.; Janner, M.; Du, Y.; Kostrikov, I.; and Levine, S. 2023. Training diffusion models with reinforcement learning. *arXiv preprint arXiv:2305.13301*.

Chang, H.; Zhang, H.; Barber, J.; Maschinot, A.; Lezama, J.; Jiang, L.; Yang, M.-H.; Murphy, K.; Freeman, W. T.; Rubinstein, M.; et al. 2023. Muse: Text-to-image generation via masked generative transformers. *arXiv preprint arXiv:2301.00704*.

Chang, H.; Zhang, H.; Jiang, L.; Liu, C.; and Freeman, W. T. 2022. Maskgit: Masked generative image transformer. In *Proceedings of the IEEE/CVF conference on computer vision and pattern recognition*, 11315–11325.

Chen, M.; Laina, I.; and Vedaldi, A. 2024. Training-free layout control with cross-attention guidance. In *Proceedings of the IEEE/CVF winter conference on applications of computer vision*, 5343–5353.

Chen, X.; Wu, Z.; Liu, X.; Pan, Z.; Liu, W.; Xie, Z.; Yu, X.; and Ruan, C. 2025a. Janus-pro: Unified multimodal understanding and generation with data and model scaling. *arXiv preprint arXiv:2501.17811*.

Chen, Y.; Ma, Z.; Jia, G.; Jiang, C.; Li, J.; and Zhou, B. 2025b. Context-Aware Autoregressive Models for Multi-Conditional Image Generation. *arXiv preprint arXiv:2505.12274*.

Cheng, B.; Ma, Y.; Wu, L.; Liu, S.; Ma, A.; Wu, X.; Leng, D.; and Yin, Y. 2024. Hico: Hierarchical controllable diffusion model for layout-to-image generation. *arXiv preprint arXiv:2410.14324*.

Chung, J.; Hyun, S.; Kim, H.; Koh, E.; Lee, M.; and Heo, J.-P. 2025. Fine-Tuning Visual Autoregressive Models for Subject-Driven Generation. *arXiv preprint arXiv:2504.02612*.

Clark, K.; Vicol, P.; Swersky, K.; and Fleet, D. J. 2023. Directly fine-tuning diffusion models on differentiable rewards. *arXiv preprint arXiv:2309.17400*.

Cui, X.; Sun, Q.; Wang, M.; Li, L.; Zhou, W.; and Li, H. 2025. LayoutEnc: Leveraging Enhanced Layout Representations for Transformer-based Complex Scene Synthesis. *ACM Transactions on Multimedia Computing, Communications and Applications*, 21(4): 1–21.

Dahary, O.; Patashnik, O.; Aberman, K.; and Cohen-Or, D. 2024. Be yourself: Bounded attention for multi-subject text-to-image generation. In *European Conference on Computer Vision*, 432–448. Springer.

Deng, H.; Pan, T.; Diao, H.; Luo, Z.; Cui, Y.; Lu, H.; Shan, S.; Qi, Y.; and Wang, X. 2024. Autoregressive video generation without vector quantization. *arXiv preprint arXiv:2412.14169*.

Esser, P.; Rombach, R.; and Ommer, B. 2021. Taming transformers for high-resolution image synthesis. In *Proceedings of the IEEE/CVF conference on computer vision and pattern recognition*, 12873–12883.

Feng, Y.; Gong, B.; Chen, D.; Shen, Y.; Liu, Y.; and Zhou, J. 2024. Ranni: Taming text-to-image diffusion for accurate instruction following. In *Proceedings of the IEEE/CVF Conference on Computer Vision and Pattern Recognition*, 4744–4753.

Ge, M.; Jia, X.; Isobe, T.; Li, X.; Wang, Q.; Mu, J.; Zhou, D.; Wang, L.; Lu, H.; Tian, L.; et al. 2024. Customizing text-to-image generation with inverted interaction. In *Proceedings of the 32nd ACM International Conference on Multimedia*, 10901–10909.

Heusel, M.; Ramsauer, H.; Unterthiner, T.; Nessler, B.; and Hochreiter, S. 2017. Gans trained by a two time-scale update rule converge to a local nash equilibrium. *Advances in neural information processing systems*, 30.

Hu, E. J.; Shen, Y.; Wallis, P.; Allen-Zhu, Z.; Li, Y.; Wang, S.; Wang, L.; Chen, W.; et al. 2022. Lora: Low-rank adaptation of large language models. *ICLR*, 1(2): 3.

Jia, C.; Luo, M.; Dang, Z.; Dai, G.; Chang, X.; Wang, M.; and Wang, J. 2024. Ssmg: Spatial-semantic map guided diffusion model for free-form layout-to-image generation. In *Proceedings of the AAAI Conference on Artificial Intelligence*, volume 38, 2480–2488.

Jiang, D.; Guo, Z.; Zhang, R.; Zong, Z.; Li, H.; Zhuo, L.; Yan, S.; Heng, P.-A.; and Li, H. 2025. T2i-r1: Reinforcing image generation with collaborative semantic-level and token-level cot. *arXiv preprint arXiv:2505.00703*.

Kirstain, Y.; Polyak, A.; Singer, U.; Matiana, S.; Penna, J.; and Levy, O. 2023. Pick-a-pic: An open dataset of user preferences for text-to-image generation. *Advances in neural information processing systems*, 36: 36652–36663.

Lee, Y.; Yoon, T.; and Sung, M. 2024. Groundit: Grounding diffusion transformers via noisy patch transplantation. *Advances in Neural Information Processing Systems*, 37: 58610–58636.

Li, T.; Tian, Y.; Li, H.; Deng, M.; and He, K. 2024a. Autoregressive image generation without vector quantization. *Advances in Neural Information Processing Systems*, 37: 56424–56445.

Li, X.; Liu, Y.; Isobe, T.; Jia, X.; Cui, Q.; Zhou, D.; Li, D.; He, Y.; Lu, H.; Wang, Z.; et al. 2025. Reneg: Learning negative embedding with reward guidance. In *Proceedings of the Computer Vision and Pattern Recognition Conference*, 23636–23645.

Li, X.; Qiu, K.; Chen, H.; Kuen, J.; Lin, Z.; Singh, R.; and Raj, B. 2024b. Controlvar: Exploring controllable visual autoregressive modeling. *arXiv preprint arXiv:2406.09750*.

Li, Y.; Liu, H.; Wu, Q.; Mu, F.; Yang, J.; Gao, J.; Li, C.; and Lee, Y. J. 2023. Gligen: Open-set grounded text-to-image

generation. In *Proceedings of the IEEE/CVF conference on computer vision and pattern recognition*, 22511–22521.

Li, Z.; Cheng, T.; Chen, S.; Sun, P.; Shen, H.; Ran, L.; Chen, X.; Liu, W.; and Wang, X. 2024c. Controlar: Controllable image generation with autoregressive models. *arXiv preprint arXiv:2410.02705*.

Liu, J.; Liu, G.; Liang, J.; Li, Y.; Liu, J.; Wang, X.; Wan, P.; Zhang, D.; and Ouyang, W. 2025. Flow-grpo: Training flow matching models via online rl. *arXiv preprint arXiv:2505.05470*.

Loshchilov, I.; and Hutter, F. 2017. Decoupled weight decay regularization. *arXiv preprint arXiv:1711.05101*.

Mu, J.; Vasconcelos, N.; and Wang, X. 2025. Editar: Unified conditional generation with autoregressive models. In *Proceedings of the Computer Vision and Pattern Recognition Conference*, 7899–7909.

Radford, A.; Kim, J. W.; Hallacy, C.; Ramesh, A.; Goh, G.; Agarwal, S.; Sastry, G.; Askell, A.; Mishkin, P.; Clark, J.; et al. 2021. Learning transferable visual models from natural language supervision. In *International conference on machine learning*, 8748–8763. PmLR.

Rafailov, R.; Sharma, A.; Mitchell, E.; Manning, C. D.; Ermon, S.; and Finn, C. 2023. Direct preference optimization: Your language model is secretly a reward model. *Advances in neural information processing systems*, 36: 53728–53741.

Ramesh, A.; Pavlov, M.; Goh, G.; Gray, S.; Voss, C.; Radford, A.; Chen, M.; and Sutskever, I. 2021. Zero-shot text-to-image generation. In *International conference on machine learning*, 8821–8831. Pmlr.

Salimans, T.; Goodfellow, I.; Zaremba, W.; Cheung, V.; Radford, A.; and Chen, X. 2016. Improved techniques for training gans. *Advances in neural information processing systems*, 29.

Shao, Z.; Wang, P.; Zhu, Q.; Xu, R.; Song, J.; Bi, X.; Zhang, H.; Zhang, M.; Li, Y.; Wu, Y.; et al. 2024. Deepseekmath: Pushing the limits of mathematical reasoning in open language models. *arXiv preprint arXiv:2402.03300*.

Sun, P.; Jiang, Y.; Chen, S.; Zhang, S.; Peng, B.; Luo, P.; and Yuan, Z. 2024. Autoregressive model beats diffusion: Llama for scalable image generation. *arXiv preprint arXiv:2406.06525*.

Tian, K.; Jiang, Y.; Yuan, Z.; Peng, B.; and Wang, L. 2024. Visual autoregressive modeling: Scalable image generation via next-scale prediction. *Advances in neural information processing systems*, 37: 84839–84865.

Touvron, H.; Lavril, T.; Izacard, G.; Martinet, X.; Lachaux, M.-A.; Lacroix, T.; Rozière, B.; Goyal, N.; Hambro, E.; Azhar, F.; et al. 2023. Llama: Open and efficient foundation language models. *arXiv preprint arXiv:2302.13971*.

Wallace, B.; Dang, M.; Rafailov, R.; Zhou, L.; Lou, A.; Purushwalkam, S.; Ermon, S.; Xiong, C.; Joty, S.; and Naik, N. 2024. Diffusion model alignment using direct preference optimization. In *Proceedings of the IEEE/CVF Conference on Computer Vision and Pattern Recognition*, 8228–8238.

Wang, J.; Tian, Z.; Wang, X.; Zhang, X.; Huang, W.; Wu, Z.; and Jiang, Y.-G. 2025. Simplear: Pushing the frontier of autoregressive visual generation through pretraining, sft, and rl. *arXiv preprint arXiv:2504.11455*.

Wang, Q.; Liu, L.; Hua, M.; Zhu, P.; Zuo, W.; Hu, Q.; Lu, H.; and Cao, B. 2022. Hs-diffusion: Semantic-mixing diffusion for head swapping. *arXiv preprint arXiv:2212.06458*.

Wang, X.; Darrell, T.; Rambhatla, S. S.; Girdhar, R.; and Misra, I. 2024a. Instancediffusion: Instance-level control for image generation. In *Proceedings of the IEEE/CVF conference on computer vision and pattern recognition*, 6232–6242.

Wang, X.; Zhang, X.; Luo, Z.; Sun, Q.; Cui, Y.; Wang, J.; Zhang, F.; Wang, Y.; Li, Z.; Yu, Q.; et al. 2024b. Emu3: Next-token prediction is all you need. *arXiv preprint arXiv:2409.18869*.

Wu, X.; Hao, Y.; Sun, K.; Chen, Y.; Zhu, F.; Zhao, R.; and Li, H. 2023. Human Preference Score v2: A Solid Benchmark for Evaluating Human Preferences of Text-to-Image Synthesis. *arXiv preprint arXiv:2306.09341*.

Xie, J.; Mao, W.; Bai, Z.; Zhang, D. J.; Wang, W.; Lin, K. Q.; Gu, Y.; Chen, Z.; Yang, Z.; and Shou, M. Z. 2024. Show-o: One Single Transformer to Unify Multimodal Understanding and Generation. *arXiv preprint arXiv:2408.12528*.

Xu, J.; Liu, X.; Wu, Y.; Tong, Y.; Li, Q.; Ding, M.; Tang, J.; and Dong, Y. 2023. Imagereward: Learning and evaluating human preferences for text-to-image generation. *Advances in Neural Information Processing Systems*, 36: 15903–15935.

Xue, Z.; Wu, J.; Gao, Y.; Kong, F.; Zhu, L.; Chen, M.; Liu, Z.; Liu, W.; Guo, Q.; Huang, W.; et al. 2025. DanceGRPO: Unleashing GRPO on Visual Generation. *arXiv preprint arXiv:2505.07818*.

Yang, A.; Li, A.; Yang, B.; Zhang, B.; Hui, B.; Zheng, B.; Yu, B.; Gao, C.; Huang, C.; Lv, C.; et al. 2025. Qwen3 technical report. *arXiv preprint arXiv:2505.09388*.

Yang, L.; Yu, Z.; Meng, C.; Xu, M.; Ermon, S.; and Cui, B. 2024. Mastering text-to-image diffusion: Recaptioning, planning, and generating with multimodal llms. In *Forty-first International Conference on Machine Learning*.

Yang, Z.; Liu, D.; Wang, C.; Yang, J.; and Tao, D. 2022. Modeling image composition for complex scene generation. In *Proceedings of the IEEE/CVF Conference on Computer Vision and Pattern Recognition*, 7764–7773.

Yao, Z.; Li, J.; Zhou, Y.; Liu, Y.; Jiang, X.; Wang, C.; Zheng, F.; Zou, Y.; and Li, L. 2024. Car: Controllable autoregressive modeling for visual generation. *arXiv preprint arXiv:2410.04671*.

Yu, J.; Li, X.; Koh, J. Y.; Zhang, H.; Pang, R.; Qin, J.; Ku, A.; Xu, Y.; Baldridge, J.; and Wu, Y. 2021. Vector-quantized image modeling with improved vqgan. *arXiv preprint arXiv:2110.04627*.

Yu, L.; Lezama, J.; Gundavarapu, N. B.; Versari, L.; Sohn, K.; Minnen, D.; Cheng, Y.; Birodkar, V.; Gupta, A.; Gu, X.; et al. 2023. Language Model Beats Diffusion–Tokenizer is Key to Visual Generation. *arXiv preprint arXiv:2310.05737*.

Zhang, H.; Hong, D.; Wang, Y.; Shao, J.; Wu, X.; Wu, Z.; and Jiang, Y.-G. 2024. Creatilayout: Siamese multimodal

diffusion transformer for creative layout-to-image generation. *arXiv preprint arXiv:2412.03859*.

Zhang, L.; Rao, A.; and Agrawala, M. 2023. Adding conditional control to text-to-image diffusion models. In *Proceedings of the IEEE/CVF international conference on computer vision*, 3836–3847.

Zhou, D.; Li, Y.; Ma, F.; Zhang, X.; and Yang, Y. 2024. Migc: Multi-instance generation controller for text-to-image synthesis. In *Proceedings of the IEEE/CVF conference on computer vision and pattern recognition*, 6818–6828.